









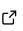


# BurnMan – a Python toolkit for planetary geophysics, geochemistry and thermodynamics

Robert Myhill <sup>1</sup><sup>2</sup>, Timo Heister <sup>3</sup>, Ian Rose<sup>4</sup>, Cayman Unterborn <sup>5</sup>, Juliane Dannberg <sup>6</sup>, and Rene Gassmoeller <sup>6</sup>

1 University of Bristol, UK 2 University of Cambridge, UK 3 Clemson University, USA 4 Independent Researcher, USA 5 Southwest Research Institute, USA 6 University of Florida, USA  Corresponding author

DOI: [10.21105/joss.05389](https://doi.org/10.21105/joss.05389)

## Software

- [Review](#) 
- [Repository](#) 
- [Archive](#) 

Editor: [Jed Brown](#)  

## Reviewers:

- [@simonwmatthews](#)
- [@kaylai](#)

Submitted: 23 September 2022

Published: 11 July 2023

## License

Authors of papers retain copyright and release the work under a Creative Commons Attribution 4.0 International License ([CC BY 4.0](https://creativecommons.org/licenses/by/4.0/)).

## Summary

Many branches of physics, chemistry and Earth sciences build complex materials from simpler constructs: rocks are composites made up of one or more phases; phases are solutions of more than one endmember; and endmembers are usually mixtures of more than one element. The properties of the endmember building blocks at different pressures and temperatures can be modelled using a wide array of different equations of state. There are also many models for the averaging of endmember properties within solutions and composite materials. Once calculated, the physical properties of composite materials can be used in many different ways.

BurnMan is an open source, extensible mineral physics module written in Python. It implements several different methods to calculate the physical properties of natural materials. The toolbox has a class-based, modular design that allows users to calculate many low-level properties that are not easily accessed using existing codes, and to combine various tools in novel, creative ways. The module includes:

- over a dozen static and thermal equations of state for pure phases;
- commonly-used solution model formalisms (ideal, (a)symmetric, subregular) and a formalism that allows users to define their own excess energy functions;
- popular endmember and solution datasets for solids and melts, including Holland & Powell (2011), de Koker et al. (2013) and Stixrude & Lithgow-Bertelloni (2021);
- an anisotropic equation of state (Myhill, 2022);
- a consistent method for combining phases into a composite assemblage, with seismic averaging schemes including Voigt, Reuss, Voigt-Reuss-Hill and the Hashin-Shtrikman bounds;
- a common set of methods to output thermodynamic and thermoelastic properties for all materials;
- a solver to chemically equilibrate composite materials;
- optimal least squares fitting routines for multivariate experimental data with (potentially correlated) errors. These allow (for example) simultaneous fitting of pure phase and solution model parameters to experimental volumes, seismic velocities and enthalpies of formation;
- “Planet” and “Layer” classes that self-consistently calculate gravity, pressure, density, mass, moment of inertia and seismic velocity profiles given chemical, thermal and dynamic constraints;
- geothermal profiles from the literature as well as the option to calculate adiabatic profiles based on mineral assemblage;
- a set of high-level functions which create files readable by seismological and geodynamic software, including: Mineos (Masters et al., 2011), AxiSEM (Nissen-Meyer et al., 2014) and ASPECT (Bangerth et al., 2022a, 2022b; Kronbichler et al., 2012); and

- a Composition class, which provides a framework to convert between mass, molar, and elemental compositions, convert to different chemical component systems, and add or subtract components.

The project includes over 40 annotated examples, an extensive suite of unit tests and benchmarks, and a directory containing user-contributed code from published papers. A multipart tutorial illustrates key functionality, including the functions required to create the figures in this paper (<https://burnman.readthedocs.io/en/latest/tutorial.html>). Using BurnMan requires only moderate Python skills, and its modular nature means that it can easily be customised.

## Statement of need

Earth, planetary and materials scientists are interested in a number of different material properties, including seismic velocities, densities and heat capacities as functions of pressure and temperature. Many of these properties are connected to each other by physical laws such as Maxwell's relations. Building models of individual phases to compute these properties can be time-consuming and prone to error. It is desirable to have well-tested and benchmarked software that makes it easy to calculate the properties of complex composite materials from existing models, and to parameterize new models from experimental data. Furthermore, there are many common scientific workflows that require thermodynamic and thermoelastic properties as input. These are the needs satisfied by the BurnMan module.

## The BurnMan project

The focus of BurnMan was originally on the seismic properties of the lower mantle (Cottaar, Heister, et al., 2014). Its scope has now expanded to encompass the thermodynamic and thermoelastic properties of any geological and planetary materials (see <https://github.com/geodynamics/burnman/releases> for the history of improvements). Pure phase equations of state are designed to be sufficiently flexible to model real-world materials from the Earth's core to the shallowest parts of the crust (e.g. Figure 1). Solution model formulations with varying levels of non-ideality are included (e.g. Figure 2), including both Gibbs and Helmholtz formulations (Myhill, 2018). Functions are provided to convert solution models from one endmember basis to another (Myhill & Connolly, 2021). A Composite class allows calculation of the properties of assemblages containing several phases and includes several seismic averaging schemes.

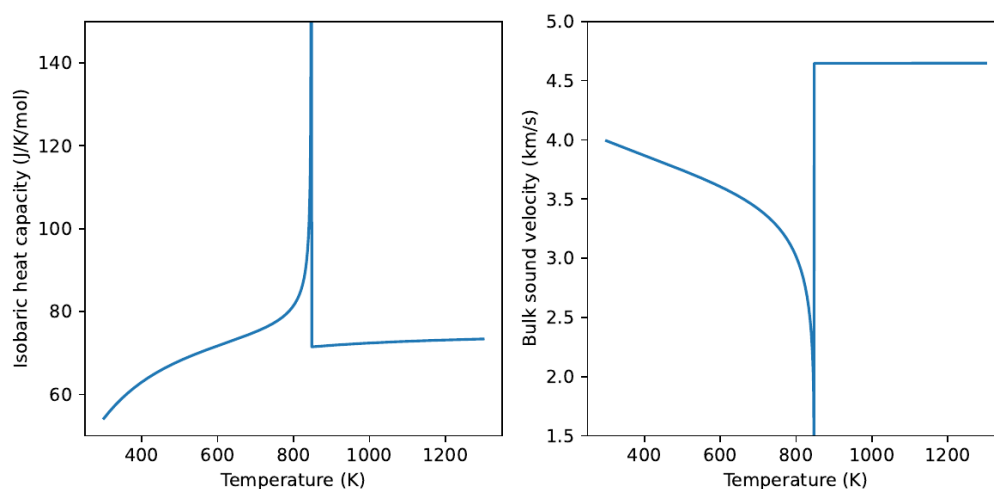


**Figure 1:** Heat capacity and bulk sound velocities of quartz through the alpha-beta quartz transition as found in (Stixrude & Lithgow-Bertelloni, 2011). This transition is modelled via a Landau-type model.

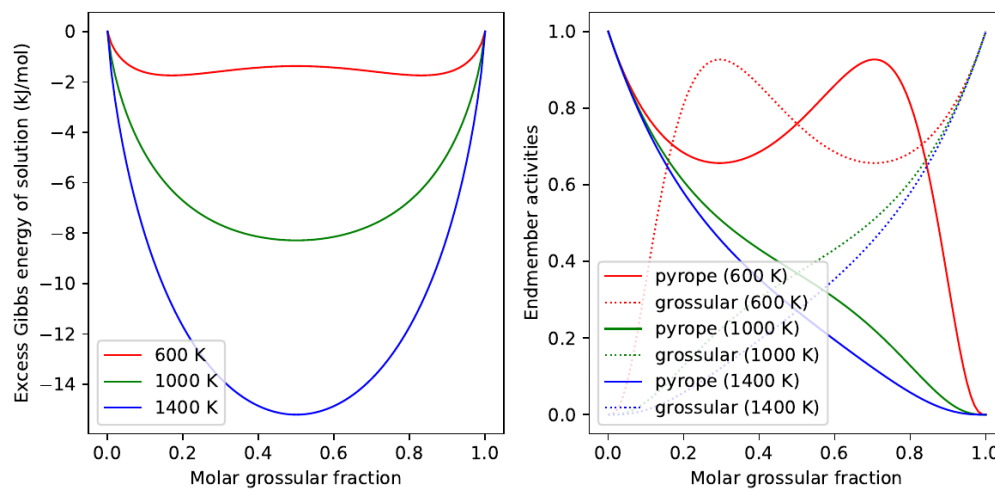


**Figure 2:** Properties of pyrope-grossular garnet at 1 GPa according to a published model (Jennings & Holland, 2015), as output by BurnMan. The excess Gibbs energy is useful for calculating phase equilibria by Gibbs minimization, while the endmember activities can be used to determine equilibrium via the equilibrium relations (Holland & Powell, 1998).

BurnMan also includes planetary Layer and Planet classes that can be used to construct planetary models with self-consistent pressure, gravity and density profiles and calculate seismic properties through those bodies. Figure 3 shows the output from a model that resembles Earth. Tools are provided to compare predicted seismic properties with published seismic models of the Earth, and to produce input files to compute synthetic seismic data using other codes, including AxiSEM (Nissen-Meyer et al., 2014) and Mineos (Masters et al., 2011; Woodhouse, 1988).

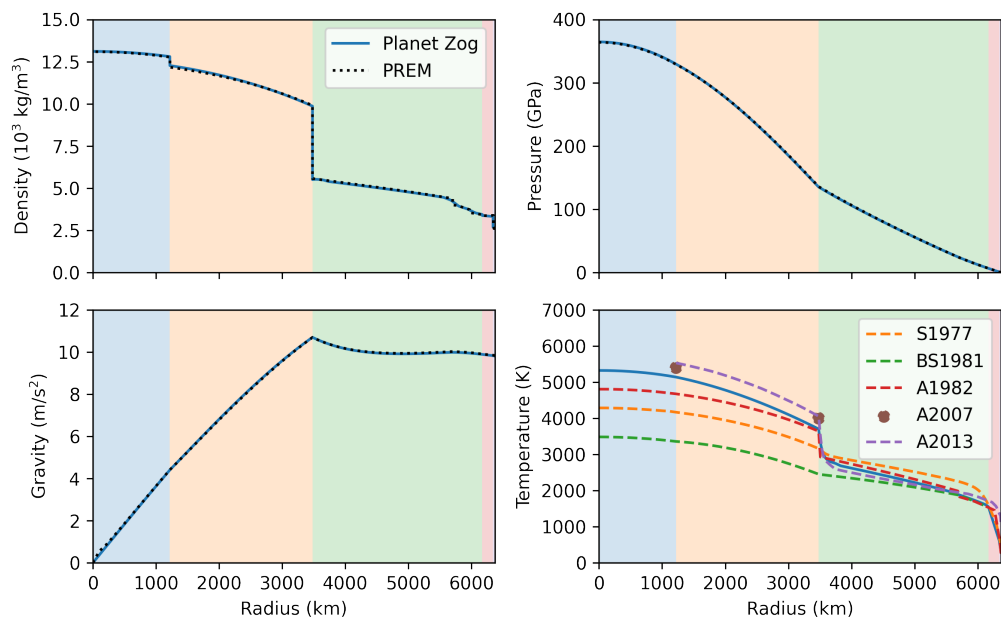


**Figure 3:** A 1D profile through Planet Zog, a planet much like Earth, with an inner and outer core (blue and orange layers), isentropic convecting lower and upper mantle (green and red), and a depleted lithosphere (lilac) split into mantle and crust. The mineralogy/composition of each layer is chosen by the user. Zog has the same mass ( $5.972e+24$  kg) and moment of inertia factor (0.3307) as Earth. BurnMan ensures that the gravity and pressure profiles satisfy hydrostatic equilibrium, and allows different layers to have different thermal profiles, including an isentropic profile with thermal boundary layers (shown here for the upper mantle, lower mantle and for the core). Depth dependent changes to density, gravity, pressure (solid blue lines) are compared with the Preliminary Reference Earth Model (PREM; dotted orange line, (Dziewonski & Anderson, 1981)). The computed geotherm is compared to several from the literature (Alfe et al., 2007; Anderson, 1982; Anzellini et al., 2013; Brown & Shankland, 1981; Stacey, 1977).

BurnMan also includes many utility functions. These include functions that fit parameters for pure phase and solution models to experimental data including full error propagation (Figure 4). Other fitting functions include `fit_composition_to_solution()` and `fit_phase_proportions_to_bulk_composition()` that use weighted constrained least squares using `cvxpy` (Diamond & Boyd, 2016) to estimate endmember or phase proportions given a bulk composition. These fitting functions apply appropriate non-negativity constraints (i.e. that no species can have negative proportions on a site, and that no phase can have a negative abundance in the bulk). An example of `fit_phase_proportions_to_bulk_composition()` that uses real experimental data (Bertka & Fei, 1997) is shown in Figure 5. Loss of an independent component from the bulk composition can be tested by adding another phase with the composition of that component (e.g. Fe) and checking that the amount of that phase is zero within uncertainties.

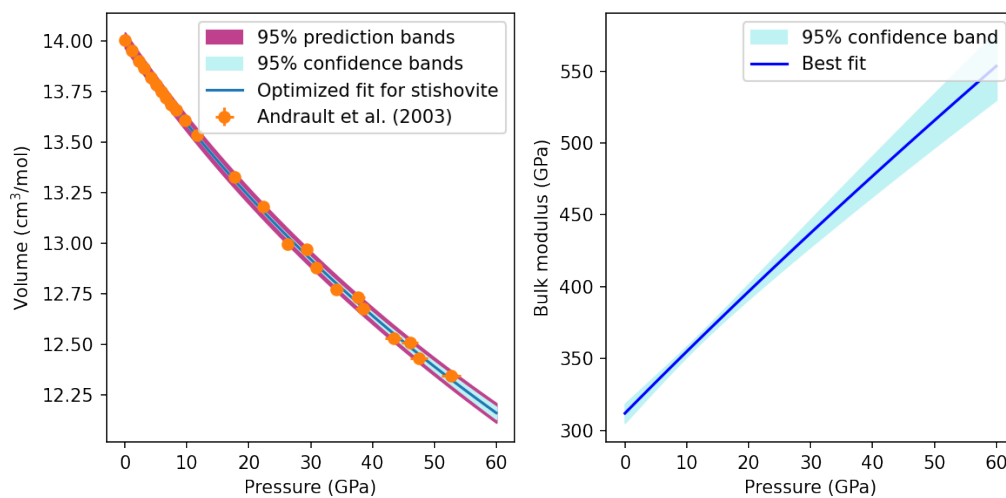


**Figure 4:** Optimized fit of a PV equation of state (Holland & Powell, 2011) to stishovite data (Andraut et al., 2003), including 95% confidence intervals on both the volume and the bulk modulus.

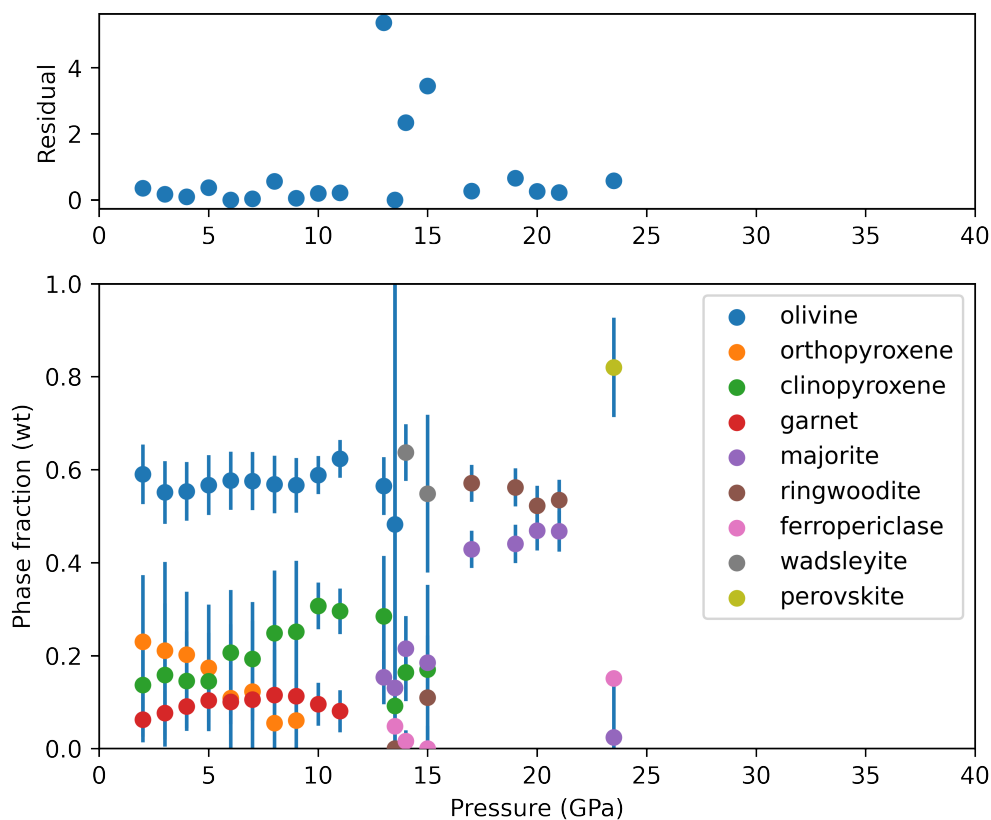


**Figure 5:** Mineral phase proportions in the mantle of Mars, estimated by using the method of constrained least squares on high pressure experimental data (Bertka & Fei, 1997). Weighted residuals (misfits) are also shown, indicating that the majority of experimental run products are consistent with the reported starting composition.

BurnMan does not attempt to replicate Gibbs minimization codes, of which there are many, such

as PerpleX (Connolly, 2009), MELTS (Ghiorso & Sack, 1995), MageMin (Riel et al., 2022), TheriakDomino (Capitani & Petrakakis, 2010), HeFESTo (Stixrude & Lithgow-Bertelloni, 2021) and FactSAGE (Bale et al., 2002). Instead, it provides two methods to deal with the problem of thermodynamic equilibrium: (1) reading in a pressure-temperature table of precalculated properties into a Material class that allows derivative properties to be calculated, and (2) a function called `equilibrate()` that equilibrates a known assemblage under user-defined constraints. This function requires an assemblage (e.g. olivine, garnet and orthopyroxene), a starting bulk composition, desired equality constraints, and optionally one or more compositional degrees of freedom. The `equilibrate` function solves the equilibrium relations (Holland & Powell, 1998) using a damped Newton root finder (Nowak & Weimann, 1991).

The `equilibrate()` function allows the user to select from a number of equality constraints, including fixed pressure, temperature, entropy or volume, or compositional equalities such as a fixed molar fraction of a phase, or a certain ratio of Mg and Fe on a particular site. The number of constraints required is two at fixed bulk composition, and one more for each degree of compositional freedom. An example of the use of the `equilibrate` function is shown in Figure 6. Full details may be found in the manual and tutorial.

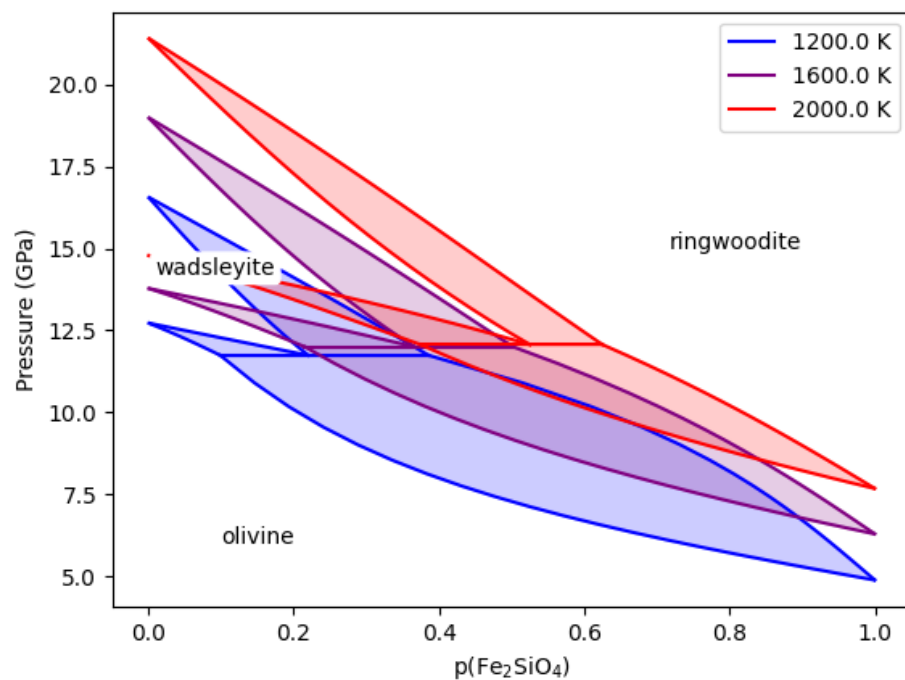


**Figure 6:** The olivine phase diagram at three different temperatures as computed using the `equilibrate` routines in BurnMan. The solution model properties are taken from the literature (Stixrude & Lithgow-Bertelloni, 2011).

## Past and ongoing research projects

In addition to mantle studies (Ballmer et al., 2017; Cottaar, Li, et al., 2014; Houser et al., 2020; Jenkins et al., 2017; Thomson et al., 2019), BurnMan has been used to investigate Earth's core (Irving et al., 2018), in phase equilibria studies (Ishii et al., 2019; Myhill et al., 2017), to develop new models for anisotropic thermodynamics (Myhill, 2022), to constrain the interiors of exoplanets (Unterborn et al., 2016; Unterborn & Panero, 2019), and to provide

input for geodynamic simulations (Dannberg et al., 2021; Heister et al., 2017).

## Acknowledgments

BurnMan was initiated at, and follow-up research support was received through, CIDER (NSF FESD grant 1135452). The authors have been supported by the Computational Infrastructure for Geodynamics initiative (CIG), through the National Science Foundation (U.S.) under Award No. EAR-0949446. They have also received support from The University of California-Davis.

Robert Myhill was supported by the Science and Technologies Funding Council (U.K.) under Award No. ST/R001332/1 and through the Natural Environment Research Council (U.K.) Large Grant MC-squared (Award No. NE/T012633/1). He would also like to thank M. Ghiorso for useful discussions and B. Watterson for the concept of Planet Zog.

Sanne Cottaar has received funding from the European Research Council (ERC) under the European Union's Horizon 2020 research and innovation programme (ZoomDeep; Award No. 804071). This funding covered collaborative visits.

Timo Heister was partially supported by NSF Award DMS-2028346, OAC-2015848, EAR-1925575, and by the Computational Infrastructure in Geodynamics initiative (CIG), through the NSF under Award EAR-0949446 and EAR-1550901 and The University of California – Davis.

Rene Gassmoeller and Juliane Dannberg were supported by NSF Awards EAR-1925677 and EAR-2054605, and by the Computational Infrastructure for Geodynamics (CIG) through the NSF under Award EAR-0949446 and EAR-1550901 and the University of California – Davis.

The BurnMan code has been contributed to the Computational Infrastructure for Geodynamics (CIG) and is hosted at [geodynamics.org](http://geodynamics.org).

## References

- Alfe, D., Gillan, M. J., & Price, G. D. (2007). Temperature and composition of the Earth's core. *Contemporary Physics*, 48(2), 63–80. <https://doi.org/10.1080/00107510701529653>
- Anderson, O. L. (1982). The Earth's core and the phase diagram of iron. *Philos. T. Roy. Soc. A*, 306(1492), 21–35. <https://doi.org/10.1098/rsta.1982.0063>
- Andrault, D., Angel, R. J., Mosenfelder, J. L., & Le Bihan, T. (2003). Equation of state of stishovite to lower mantle pressures. *American Mineralogist*, 88(2-3), 301–307. <https://doi.org/10.2138/am-2003-2-307>
- Anzellini, S., Dewaele, A., Mezouar, M., Loubeyre, P., & Morard, G. (2013). Melting of iron at Earth's inner core boundary based on fast X-ray diffraction. *Science*, 340(6131), 464–466. <https://doi.org/10.1126/science.1233514>
- Bale, C. W., Chartrand, P., Degterov, S. A., Eriksson, G., Hack, K., Ben Mahfoud, R., Melançon, J., Pelton, A. D., & Petersen, S. (2002). FactSage thermochemical software and databases. *Calphad*, 26(2), 189–228. [https://doi.org/10.1016/S0364-5916\(02\)00035-4](https://doi.org/10.1016/S0364-5916(02)00035-4)
- Ballmer, M. D., Houser, C., Hernlund, J. W., Wentzcovitch, R. M., & Hirose, K. (2017). Persistence of strong silica-enriched domains in the Earth's lower mantle. *Nature Geoscience*, 10(3), 236–240. <https://doi.org/10.1038/ngeo2898>
- Bangerth, W., Dannberg, J., Fraters, M., Gassmoeller, R., Glerum, A., Heister, T., Myhill, R., & Naliboff, J. (2022a). ASPECT: *Advanced Solver for Problems in Earth's ConvecTion, User Manual*. <https://doi.org/10.6084/m9.figshare.4865333>



- Bangerth, W., Dannberg, J., Fraters, M., Gassmoeller, R., Glerum, A., Heister, T., Myhill, R., & Naliboff, J. (2022b). *ASPECT v2.4.0* (Version v2.4.0). Zenodo. <https://doi.org/10.5281/zenodo.6903424>
- Bertka, C. M., & Fei, Y. (1997). Mineralogy of the Martian interior up to core-mantle boundary pressures. *Journal of Geophysical Research: Solid Earth*, *102*(B3), 5251–5264. <https://doi.org/10.1029/96JB03270>
- Brown, J., & Shankland, T. (1981). Thermodynamic parameters in the Earth as determined from seismic profiles. *Geophys. J. Int.*, *66*(3), 579–596. <https://doi.org/10.1111/j.1365-246X.1981.tb04891.x>
- Capitani, C. de, & Petrakakis, K. (2010). The computation of equilibrium assemblage diagrams with Theriak/Domino software. *American Mineralogist*, *95*(7), 1006–1016. <https://doi.org/10.2138/am.2010.3354>
- Connolly, J. A. D. (2009). The geodynamic equation of state: What and how. *Geochemistry, Geophysics, Geosystems*, *10*(10). <https://doi.org/10.1029/2009GC002540>
- Cottaar, S., Heister, T., Rose, I., & Unterborn, C. T. (2014). BurnMan: A lower mantle mineral physics toolkit. *Geochemistry, Geophysics, Geosystems*, *15*(4), 1164–1179. <https://doi.org/10.1002/2013GC005122>
- Cottaar, S., Li, M., McNamara, A. K., Romanowicz, B., & Wenk, H.-R. (2014). Synthetic seismic anisotropy models within a slab impinging on the core–mantle boundary. *Geophysical Journal International*, *199*(1), 164–177. <https://doi.org/10.1093/gji/ggu244>
- Dannberg, J., Myhill, R., Gassmüller, R., & Cottaar, S. (2021). The morphology, evolution and seismic visibility of partial melt at the core-mantle boundary: implications for ULVZs. *Geophysical Journal International*, *227*(2), 1028–1059. <https://doi.org/10.1093/gji/ggab242>
- de Koker, N., Karki, B. B., & Stixrude, L. (2013). Thermodynamics of the MgO-SiO<sub>2</sub> liquid system in Earth's lowermost mantle from first principles. *Earth and Planetary Science Letters*, *361*, 58–63. <https://doi.org/10.1016/j.epsl.2012.11.026>
- Diamond, S., & Boyd, S. (2016). CVXPY: A Python-Embedded Modeling Language for Convex Optimization. *arXiv e-Prints*, arXiv:1603.00943. <https://doi.org/10.48550/arXiv.1603.00943>
- Dziewonski, A. M., & Anderson, D. L. (1981). Preliminary reference Earth model. *Physics of the Earth and Planetary Interiors*, *25*(4), 297–356. [https://doi.org/10.1016/0031-9201\(81\)90046-7](https://doi.org/10.1016/0031-9201(81)90046-7)
- Ghiorso, M. S., & Sack, R. O. (1995). Chemical mass transfer in magmatic processes IV. A revised and internally consistent thermodynamic model for the interpolation and extrapolation of liquid-solid equilibria in magmatic systems at elevated temperatures and pressures. *Contributions to Mineralogy and Petrology*, *119*(2), 197–212. <https://doi.org/10.1007/BF00307281>
- Heister, T., Dannberg, J., Gassmüller, R., & Bangerth, W. (2017). High accuracy mantle convection simulation through modern numerical methods—II: realistic models and problems. *Geophysical Journal International*, *210*(2), 833–851. <https://doi.org/10.1093/gji/ggx195>
- Holland, T. J. B., & Powell, R. (1998). An internally consistent thermodynamic data set for phases of petrological interest. *Journal of Metamorphic Geology*, *16*(3), 309–343. <https://doi.org/10.1111/j.1525-1314.1998.00140.x>
- Holland, T. J. B., & Powell, R. (2011). An improved and extended internally consistent thermodynamic dataset for phases of petrological interest, involving a new equation of state for solids. *Journal of Metamorphic Geology*, *29*(3), 333–383. <https://doi.org/10.1111/j.1525-1314.2010.00923.x>



- Houser, C., Hernlund, J. W., Valencia-Cardona, J., & Wentzcovitch, R. M. (2020). Discriminating lower mantle composition. *Physics of the Earth and Planetary Interiors*, 308, 106552. <https://doi.org/10.1016/j.pepi.2020.106552>
- Irving, J. C., Cottaar, S., & Lekić, V. (2018). Seismically determined elastic parameters for Earth's outer core. *Science Advances*, 4(6), eaar2538. <https://doi.org/10.1126/sciadv.aar2538>
- Ishii, T., Huang, R., Myhill, R., Fei, H., Koemets, I., Liu, Z., Maeda, F., Yuan, L., Wang, L., Druzhbin, D., & al., et. (2019). Sharp 660-km discontinuity controlled by extremely narrow binary post-spinel transition. *Nature Geoscience*, 12(10), 869–872. <https://doi.org/10.1038/s41561-019-0452-1>
- Jenkins, J., Deuss, A., & Cottaar, S. (2017). Converted phases from sharp 1000 km depth mid-mantle heterogeneity beneath Western Europe. *Earth and Planetary Science Letters*, 459, 196–207. <https://doi.org/10.1016/j.epsl.2016.11.031>
- Jennings, E. S., & Holland, T. J. B. (2015). A simple thermodynamic model for melting of peridotite in the system NCFMASOCr. *Journal of Petrology*, 56(5), 869–892. <https://doi.org/10.1093/petrology/egv020>
- Kronbichler, M., Heister, T., & Bangerth, W. (2012). High accuracy mantle convection simulation through modern numerical methods. *Geophysical Journal International*, 191, 12–29. <https://doi.org/10.1111/j.1365-246X.2012.05609.x>
- Masters, G., Woodhouse, J. H., & Freeman, G. (2011). Mineos v1.0.2 [software]. *Computational Infrastructure for Geodynamics*, 99. <https://geodynamics.org/cig/software/mineos/>
- Myhill, R. (2018). The elastic solid solution model for minerals at high pressures and temperatures. *Contributions to Mineralogy and Petrology*, 173(2). <https://doi.org/10.1007/s00410-017-1436-z>
- Myhill, R. (2022). An anisotropic equation of state for high pressure, high temperature applications. *Geophysical Journal International*. <https://doi.org/10.1093/gji/ggac180>
- Myhill, R., & Connolly, J. A. D. (2021). Notes on the creation and manipulation of solid solution models. *Contributions to Mineralogy and Petrology*, 176(10). <https://doi.org/10.1007/s00410-021-01825-1>
- Myhill, R., Frost, D. J., & Novella, D. (2017). Hydrous melting and partitioning in and above the mantle transition zone: Insights from water-rich MgO–SiO<sub>2</sub>–H<sub>2</sub>O experiments. *Geochimica Et Cosmochimica Acta*, 200, 408–421. <https://doi.org/10.1016/j.gca.2016.05.027>
- Nissen-Meyer, T., Driel, M. van, Stähler, S. C., Hosseini, K., Hempel, S., Auer, L., Colombi, A., & Fournier, A. (2014). AxiSEM: broadband 3-D seismic wavefields in axisymmetric media. *Solid Earth*, 5(1), 425–445. <https://doi.org/10.5194/se-5-425-2014>
- Nowak, U., & Weimann, L. (1991). A family of Newton codes for systems of highly nonlinear equations. Technical Report TR-91-10. *Zuse Institute Berlin, ZIB*.
- Riel, N., Kaus, B. J. P., Green, E. C. R., & Berlie, N. (2022). MAGEMin, an efficient Gibbs energy minimizer: application to igneous systems. *Geochemistry, Geophysics, Geosystems*, 23(7), e2022GC010427. <https://doi.org/10.1029/2022GC010427>
- Stacey, F. D. (1977). A thermal model of the Earth. *Physics of the Earth and Planetary Interiors*, 15(4), 341–348. [https://doi.org/10.1016/0031-9201\(77\)90096-6](https://doi.org/10.1016/0031-9201(77)90096-6)
- Stixrude, L., & Lithgow-Bertelloni, C. (2011). Thermodynamics of mantle minerals-II. Phase equilibria. *Geophys. J. Int.*, 184(3), 1180–1213. <https://doi.org/10.1111/j.1365-246X.2010.04890.x>

- Stixrude, L., & Lithgow-Bertelloni, C. (2021). Thermal expansivity, heat capacity and bulk modulus of the mantle. *Geophysical Journal International*, 228(2), 1119–1149. <https://doi.org/10.1093/gji/ggab394>
- Thomson, A. R., Crichton, W. A., Brodholt, J. P., Wood, I. G., Siersch, N. C., Muir, J. M. R., Dobson, D. P., & Hunt, S. A. (2019). Seismic velocities of CaSiO<sub>3</sub> perovskite can explain LLSVPs in Earth's lower mantle. *Nature*, 572(7771), 643–647. <https://doi.org/10.1038/s41586-019-1483-x>
- Unterborn, C. T., Dismukes, E. E., & Panero, W. R. (2016). Scaling the Earth: a sensitivity analysis of terrestrial exoplanetary interior models. *The Astrophysical Journal*, 819(1), 32. <https://doi.org/10.3847/0004-637X/819/1/32>
- Unterborn, C. T., & Panero, W. R. (2019). The pressure and temperature limits of likely rocky exoplanets. *Journal of Geophysical Research: Planets*, 124(7), 1704–1716. <https://doi.org/10.1029/2018JE005844>
- Woodhouse, J. (1988). The calculation of the eigenfrequencies and eigenfunctions of the free oscillations of the Earth and Sun. *Seismological Algorithms: Computational Methods and Computer Programs*, 321–370.